Transverse Momentum in Nucleons

David M. Riser, Ph.D.

University of Connecticut,

Insert abstract here.

Transverse Momentum in Nucleons

David M. Riser

B.S. Physics, Delaware State University, 2013

A Dissertation

Submitted in Partial Fullfilment of the

Requirements for the Degree of

Doctor of Philosophy

at the

University of Connecticut

APPROVAL PAGE

Doctor of Philosophy Dissertation

Transverse Momentum in Nucleons

Presented by

David M. Riser,

Major Advisor

_____
Kyungseon Joo

Associate Advisor

_____
Peter Schweitzer

Associate Advisor

_____
Andrew Puckett

University of Connecticut

To all the beers that lost their lives in the making of this work.

ACKNOWLEDGEMENTS

Thanks everyone.

TABLE OF CONTENTS

LIST OF FIGURES

LIST OF TABLES

Chapter 1

Introduction

Research into the internal structure of protons and neutrons began in 1955 with the pioneering work of Hofstadter and McAllister. Working together at Standford, the pair measured the electron-proton scattering cross section with 188 MeV electrons incident on hydrogen. Their measured cross section was inconsistent with the cross section predicted for a point-like proton, demonstrating its finite size [1], [2], [3]. Simultaneously, the Brookhaven Cosmotron produced an overwhelming number of new particles, creating what was dubbed a "particle zoo". Theoretical efforts by Gell-Mann and Zwieg showed that the particle zoo could be explained by combinations of fractionally charged particles that Gell-Mann coined quarks [4].

1.1 Deeply Inelastic Scattering and Structure Functions

Learning more about quarks required scattering at higher energies. As the electron energy increases and the wavelength of the virtual photon becomes small $\lambda < r_p$ deeply inelastic scattering (DIS) occurs where the virtual photon interacts with
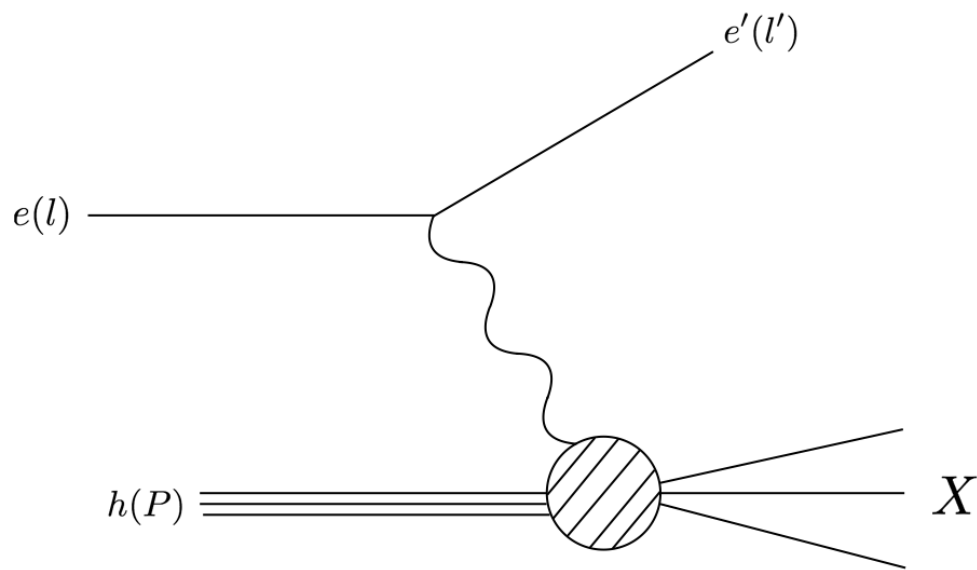
Fig. 1.1: Deeply inelastic scattering (DIS) between a lepton and a hadron, in this thesis an electron and a proton.

a constituent quark inside the proton and the proton subsequently breaks up. The cross section for DIS can be described using QED in terms of two structure functions F_1 and F_2. As we will see below, these structure functions describe quark momentum in the proton.

$$\frac{d^2\sigma}{dx dQ^2} = \frac{4\pi\alpha^2}{Q^4}\left\{\left(1 - y - \frac{m_p^2 y^2}{Q^2}\right)\frac{F_2(x, Q^2)}{x} + y^2 F_1(x, Q^2)\right\} \qquad (1.1)$$

The electron kinematics are described by the four momentum transfer $q^\mu = l^\mu - l'^\mu$ (shown in figure 1.1), the negative momentum transfer $Q^2 = -q^\mu q_\mu$ and,

$$x = \frac{Q^2}{2P \cdot q} \qquad\qquad y = \frac{P \cdot q}{P \cdot l} \qquad (1.2)$$

where x is called the momentum fraction and y is the inelasticity. The variable x (which will appear throughout this thesis) describes the fraction of the total proton momentum carried by the quark struck in the scattering. The constant α is the fine structure constant of QED. For the case that $Q^2 \gg m_p^2 y^2$ the cross section can be approximated as shown below.

$$\frac{d^2\sigma}{dx dQ^2} \approx \frac{4\pi\alpha^2}{Q^4}\left\{(1 - y)\frac{F_2(x, Q^2)}{x} + y^2 F_1(x, Q^2)\right\} \qquad (1.3)$$

First measurements of the DIS structure functions [5] showed that they are

approximately independent of Q^2 (Bjorken scaling) and that they appear to be related to each other through the Callan-Gross relation **??**.

$$F_2(x) = 2xF_1(x) \tag{1.4}$$

Both of these features are predicted by the parton model, a tool introduced by Richard Feynman in 1969 [6].

1.2 The Parton Model and Parton Distribution Functions

Feynman noted that high energy electron-proton collisions exist on a very short timescale, and can be imagined as electrons interacting electromagnetically (or electroweakly) with single quarks in the proton. Elastic electron-quark scattering is calculable, but since the quark in the proton is not free a parton distribution function $q_i(x)$ was introduced to model the quarks interaction with the other constituents of the proton (the index i refers to the quark flavor). The parton distribution functions (PDFs) describe the probability of finding a quark of flavor i in a proton (or other hadron) with momentum fraction x (this interpretation is no longer valid once the Q^2 evolution is calculated using DGLAP). By using the parton model the DIS cross section can be predicted in terms of the PDFs.

$$\frac{d^2\sigma}{dxdQ^2} = \frac{4\pi\alpha^2}{Q^4}\left\{1 - y + \frac{y^2}{2}\right\}\sum_i Q_i^2 q_i^p(x) \tag{1.5}$$
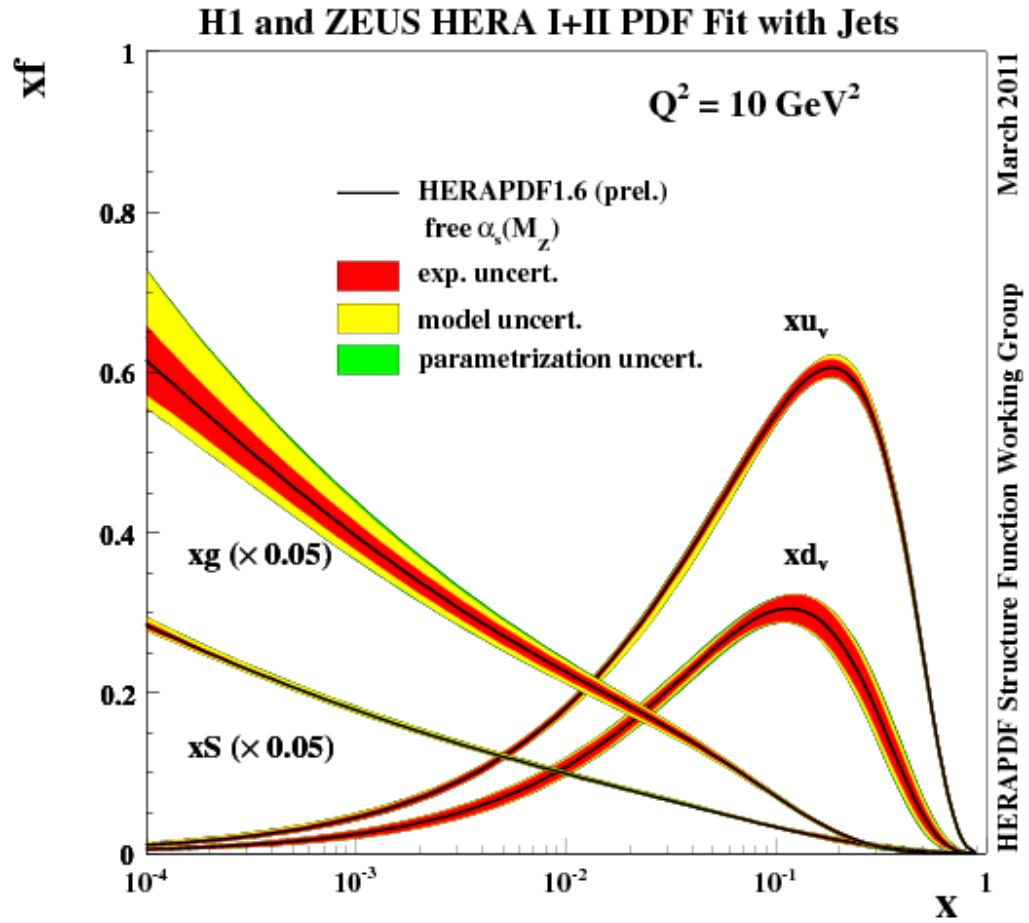
Fig. 1.2: PDFs extracted from HERA data, showing the dominance of gluons and sea quarks at lower momentum fraction x.

When equating 1.3 with 1.5 Bjorken scaling and the Callan-Gross relation are predicted by the parton model.

$$F_2(x, Q^2) = 2xF_1(x, Q^2) = x \sum_i Q_i^2 q_i^p(x) \tag{1.6}$$

These first triumphs of the parton model led to in depth studies of the structure functions at HERA.

1.3 HERA

HERA studied DIS extensively at large $Q^2 > 200 \ GeV^2$ by colliding 27.5 GeV electrons and 820 or 920 GeV protons. The H1 and ZEUS experiments mapped proton structure functions in great detail. The results 1.3 display a weak dependence on Q^2; a feature calculable using the DGLAP evolution equations. The PDFs extracted 1.2 from these structure functions show that almost half of the proton momentum is carried by gluons (and quark/anti-quark pairs). These results demonstrated that a simple picture of the proton as three valence quarks (uud) is not sufficient.

1.4 Semi-Inclusive Deeply Inelastic Scattering

DIS events where one hadron is detected in the final state are called semi-inclusive DIS (SIDIS) events. The detection of a hadron in the final state provides information needed to go beyond a discussion of quark momentum along the hard

HERA F$_2$
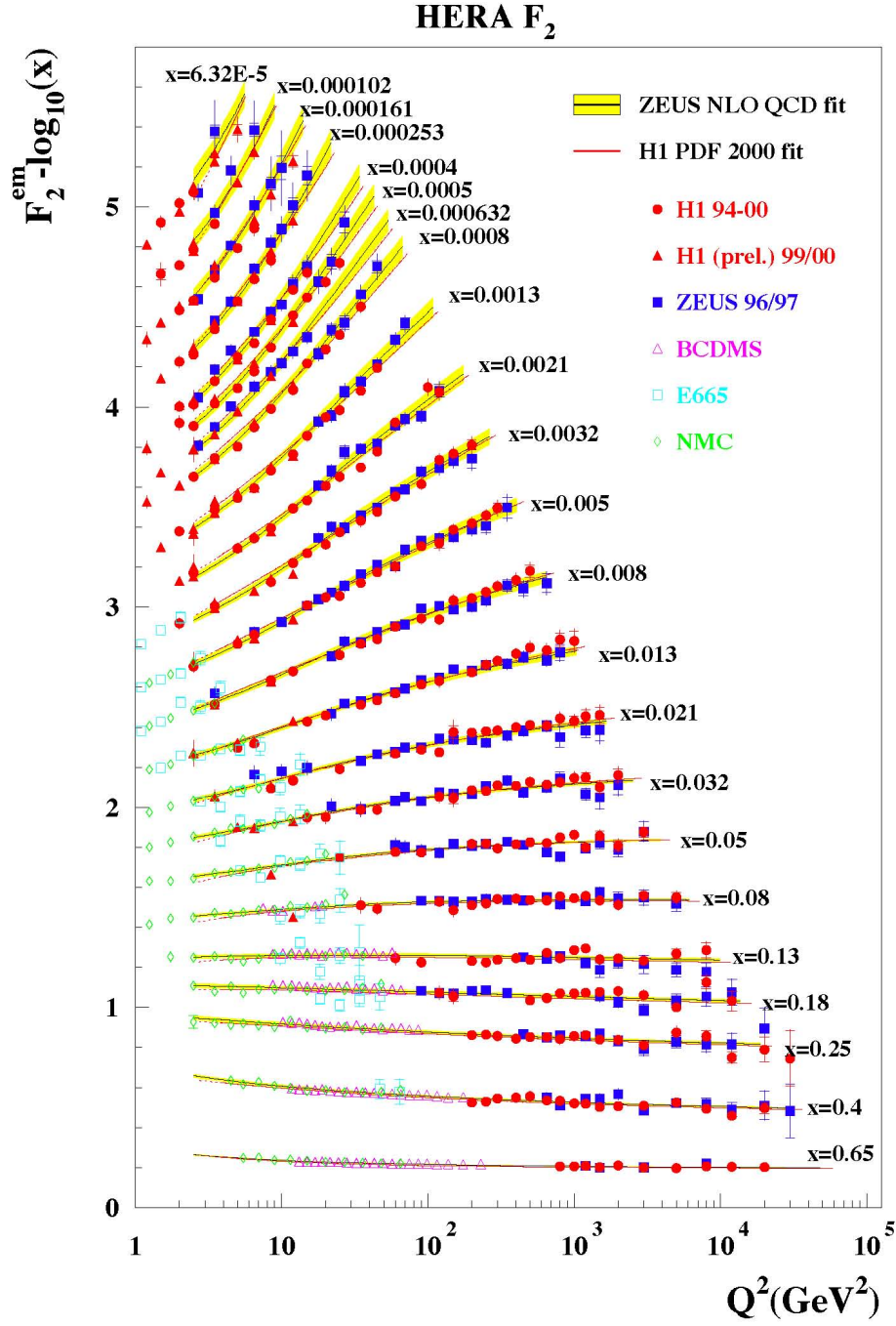
Fig. 1.3: HERA experiments ZEUS and H1 mapped out the structure function F_2, which displayed the predicted Bjorken scaling for most values of x. The mild Q^2 dependence of the PDFs can be calculated using the DGLAP evolution equations for the PDFs, providing an understanding for the observed dependence.
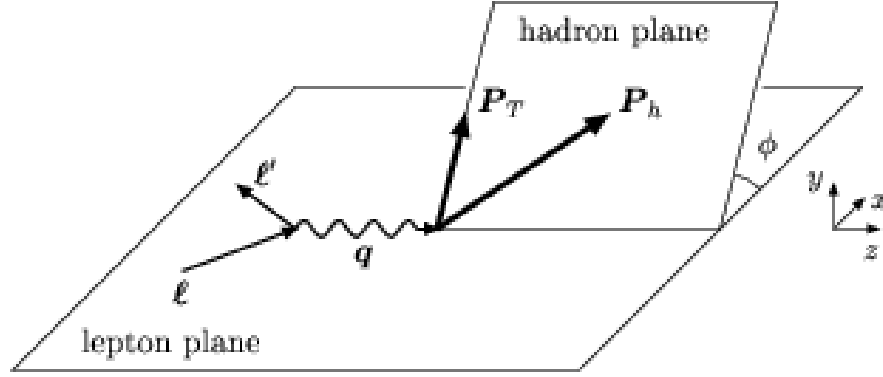
Fig. 1.4: In a SIDIS event the scattered electron is detected as well as one final state hadron, allowing for the calculation of the angle ϕ_h which appears frequently in the SIDIS cross section.

scattering direction and into the plane transverse to it. A diagrammatic representation of the reaction 1.4 shows the hadron scattering out of the lepton plane with angle ϕ (also noted ϕ_h in other places).

Analogously to the manner in which the DIS cross section can be described by structure functions, the SIDIS cross section 1.7 can be decomposed into a set of 18 structure functions (depending on the polarization direction of the electron and proton) [7], [8]. The structure functions F_{ij} are indexed by the beam polarization i and the target polarization j, which take on values of U, L, and T for unpolarized, longitudinal, and transverse respectively.

$$\frac{d\sigma}{dx \, dQ^2 \, d\psi \, dz \, d\phi_h \, dP_{h\perp}^2} =$$

$$\frac{\alpha^2 y}{4(k \cdot P) x^2 Q^2 (1-\varepsilon)} \left(1 + \frac{\gamma^2}{2x}\right) \Bigg[F_{UU,T} + \varepsilon F_{UU,L} + \sqrt{2\varepsilon(1+\varepsilon)} F_{UU}^{\cos \phi_h} \cos \phi_h$$

$$+ \varepsilon F_{UU}^{\cos(2\phi_h)} \cos(2\phi_h) + \lambda_e \sqrt{2\varepsilon(1-\varepsilon)} F_{LU}^{\sin \phi_h} \sin \phi_h$$

$$+ s_{||} \left(\sqrt{2\varepsilon(1+\varepsilon)} F_{UL}^{\sin \phi_h} \sin \phi_h + \varepsilon F_{UL}^{\sin(2\phi_h)} \sin(2\phi_h) \right)$$

$$+ \lambda_e s_{||} \left(\sqrt{1-\varepsilon^2} F_{LL} + \sqrt{2\varepsilon(1-\varepsilon)} F_{LL}^{\cos \phi_h} \cos \phi_h \right)$$

$$+ s_\perp \Bigg[\sin(\phi_h - \phi_S) \left(F_{UT,T}^{\sin(\phi_h - \phi_S)} + \varepsilon F_{UT,L}^{\sin(\phi_h - \phi_S)} \right)$$

$$+ \varepsilon F_{UT}^{\sin(\phi_h + \phi_S)} \sin(\phi_h + \phi_S) + \varepsilon F_{UT}^{\sin(3\phi_h - \phi_S)} \sin(3\phi_h - \phi_S)$$

$$+ \sqrt{2\varepsilon(1+\varepsilon)} F_{UT}^{\sin \phi_S} \sin \phi_S + \sqrt{2\varepsilon(1+\varepsilon)} F_{UT}^{\sin(2\phi_h - \phi_S)} \sin(2\phi_h - \phi_S) \Bigg]$$

$$+ s_\perp \lambda_e \Bigg[\sqrt{1-\varepsilon^2} F_{LT}^{\cos(\phi_h - \phi_S)} \cos(\phi_h - \phi_S) + \sqrt{2\varepsilon(1-\varepsilon)} F_{LT}^{\cos \phi_S} \cos \phi_S$$

$$+ \sqrt{2\varepsilon(1-\varepsilon)} F_{LT}^{\cos(2\phi_h - \phi_S)} \cos(2\phi_h - \phi_S) \Bigg] \Bigg]$$

In the SIDIS cross section the following hadronic kinematic variables are used.

$$z = \frac{P \cdot P_h}{P \cdot q} \qquad\qquad \gamma = \frac{2Mx}{Q} \qquad\qquad (1.7)$$

Additionally, the ratio ε of the longitudinal and transverse photon flux is shown below.

$$\varepsilon = \frac{1 - y - \frac{1}{4}\gamma^2 y^2}{1 - y + \frac{1}{2}y^2 + \frac{1}{4}\gamma^2 y^2} \tag{1.8}$$

By experimentally controlling the spin of the electron (λ_e) and target ($s_\perp$, $s_\parallel$) different terms of the cross section can be observed in isolation. For the remainder of this thesis our discussion will focus on unpolarized protons, reducing the number of structure functions to five.

$$\frac{d\sigma}{dx\, dQ^2\, dz\, d\phi_h\, dP_{h\perp}^2} =$$
$$\frac{\pi\alpha^2 y}{2(k \cdot P)x^2 Q^2(1-\varepsilon)} \left(1 + \frac{\gamma^2}{2x}\right) \left[F_{UU,T} + \varepsilon F_{UU,L} + \sqrt{2\varepsilon(1+\varepsilon)}F_{UU}^{\cos\phi_h} \cos\phi_h\right.$$
$$\left. + \varepsilon F_{UU}^{\cos(2\phi_h)} \cos(2\phi_h) + \lambda_e \sqrt{2\varepsilon(1-\varepsilon)}F_{LU}^{\sin\phi_h} \sin\phi_h\right]$$

The SIDIS structure functions are actively being studied for their connection to transverse momentum dependent functions.

1.5   Transverse Momentum Dependent Functions

Two types of transverse momentum dependent functions contribute to the SIDIS structure functions. The transverse momentum dependent parton distribution functions (TMD PDFs) depend on the momentum fraction x as well as the quark momentum in the transverse plane k_T, and are denoted $f^a(x, k_T^2)$. Fragmentation functions describe the probability of a quark flavor a fragmenting into the

nucleon / quark	U	L	T
U	f_1		$h_1^\perp$
L		g_{1L}	$h_{1L}^\perp$
T	$f_{1T}^\perp$	g_{1T}	$h_1,\ h_{1T}^\perp$

Fig. 1.5: Twist two PDFs. The leftmost column refers to the polarization of the nucleon, while the top row refers to the polarization of the quark inside of the nucleon. Although not explicit in the table, all of these functions depend on the quark flavor denoted elsewhere by a.

observed hadron h and are denoted by $D^a(z, p_T^2)$. At leading order (called twist-two) there are eight TMD PDFs and eight TMD FFs (see table 1.5 for a list of twist two PDFs). At twist-three an additional sixteen TMD PDFs are introduced, suppressed by a factor of M_p/Q.

In the TMD framework, the structure functions can be expressed as convolutions of PDFs and FFs. The following notation $\mathcal{C}[\omega f D]$ was introduced in [8] to simplify life.

$$\mathcal{C}[\omega f D] = x \sum_a e_a^2 \int d^2\boldsymbol{p}_T d^2\boldsymbol{k}_T \delta^{(2)}\left(z\boldsymbol{k}_T + \boldsymbol{p}_T - \boldsymbol{P}_{h\perp}\right) \omega(\boldsymbol{k}_T, \boldsymbol{p}_T) f^a(x, k_T^2) D^a(z, p_T^2)$$

(1.9)

The convolution operation is denoted by the $\mathcal{C}$ character, while the w refers to a kinematic weighting function which can be one, f is the PDF and D is the FF. Using this notation, the five structure functions appearing in the cross section are shown below.

$$F_{UU,T} = \mathcal{C}[f_1 D_1] = x \sum_a e_a^2 \int d^2\boldsymbol{p}_T d^2\boldsymbol{k}_T \delta^{(2)} \left(z\boldsymbol{k}_T + \boldsymbol{p}_T - \boldsymbol{P}_{h\perp}\right) f_1^a(x, k_T^2) D_1^a(z, p_T^2)$$

(1.10)

$$F_{UU,L} = 0$$

(1.11)

$$F_{UU}^{\cos \phi_h} = \frac{2M}{Q} \mathcal{C} \left[-\frac{\hat{\boldsymbol{h}} \cdot \boldsymbol{k}_T}{M_h} \left(x h H_1^\perp + \frac{M_h}{M} f_1 \frac{\tilde{D}^\perp}{z} \right) - \frac{\hat{\boldsymbol{h}} \cdot \boldsymbol{p}_T}{M} \left(x f^\perp D_1 + \frac{M_h}{M} h_1^\perp \frac{\tilde{H}}{z} \right) \right]$$

(1.12)

$$F_{UU}^{\cos 2\phi_h} = \mathcal{C} \left[-\frac{2(\hat{\boldsymbol{h}} \cdot \boldsymbol{k}_T)(\hat{\boldsymbol{h}} \cdot \boldsymbol{p}_T) - \boldsymbol{k}_T \cdot \boldsymbol{p}_T}{M M_h} h_1^\perp H_1^\perp \right]$$

(1.13)

$$F_{LU}^{\sin \phi} = \frac{2M}{Q} \mathcal{C} \left[-\frac{\hat{\boldsymbol{h}} \cdot \boldsymbol{k}_T}{M_h} \left(x e H_1^\perp + \frac{M_h}{M} f_1 \frac{\tilde{G}^\perp}{z} \right) + \frac{\hat{\boldsymbol{h}} \cdot \boldsymbol{p}_T}{M} \left(x g^\perp D_1 + \frac{M_h}{M} h_1^\perp \frac{\tilde{E}}{z} \right) \right]$$

(1.14)

1.5.1 Factorization Theorems

While the details of the derivation of equation 1.7 are left to the literature (see reference [7] and reference [8] for an overview), this introduction would not be complete without a mention of the importance of factorization theorems. The ability to write down structure functions in SIDIS (as well as Drell-Yan and Semi-

Inclusive Anhillation of e^+e^-) as non-perturbative TMD functions and some calculable hard scattering part is the essence of factorization theorems. Factorization has not been demonstrated for all twist, but has been demonstrated for SIDIS at leading twist (twist-two) in recent years. The most comprehensive reference on the subject is John Collins book (see [9]).

1.5.2   Unpolarized TMD

The unpolarized structure functions are measurable through the observable known as multiplicity, measured by both HERMES (27.6 GeV electrons, described in Ref. [10]) and COMPASS (160 GeV muons, described in Ref. [11]). The multiplicity of HERMES is defined below, the COMPASS definition is similar.

$$M_n^h(x_B, Q^2, z, P_T) = \frac{1}{\frac{d^2\sigma_{DIS}}{dx_B \, dQ^2}} \int_0^{2\pi} \frac{d^5\sigma_h}{dx_B \, dQ^2 dz dP_T d\phi_h} d\phi_h \qquad (1.15)$$

This can also be written in terms of the corrected yield N^h.

$$M_n^h(x_B, Q^2, z, P_T) = \frac{1}{\frac{d^2 N_{DIS}}{dx_B \, dQ^2}} \int_0^{2\pi} \frac{d^5 N^h}{dx_B \, dQ^2 dz dP_T d\phi_h} d\phi_h \qquad (1.16)$$

The unpolarized PDF f_1 and FF D_1 have been extracted from these data with good results by using Gaussian transverse momentum dependence [12]. A representative example of the results from HERMES are shown in figure 1.6, and the COMPASS results can be seen in 1.7.
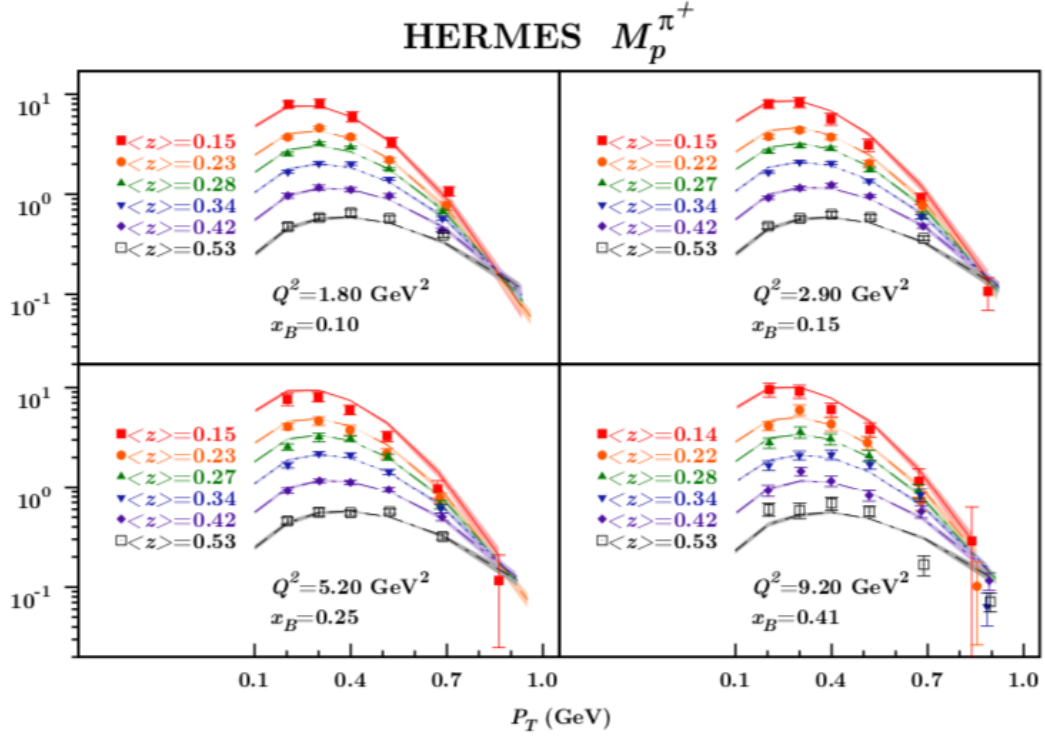
Fig. 1.6: HERMES multiplicities fit using the Gaussian ansatz. HERMES multiplicities described well by the Gaussian ansatz.

$$f_{q/p}(x, k_\perp) = f_{q/p}(x) \frac{e^{-k_\perp^2/<k_\perp^2>}}{\pi < k_\perp^2 >} \tag{1.17}$$

$$D_{h/q}(z, p_\perp) = D_{h/q}(z) \frac{e^{-p_\perp^2/<p_\perp^2>}}{\pi < p_\perp^2 >} \tag{1.18}$$

The x and z dependent parts of the TMD PDF and FF used in the fit were taken from previous fits of $f_1(x)$ the co-linear PDF and from e^+e^- scattering data to constrain $D_1(z)$.
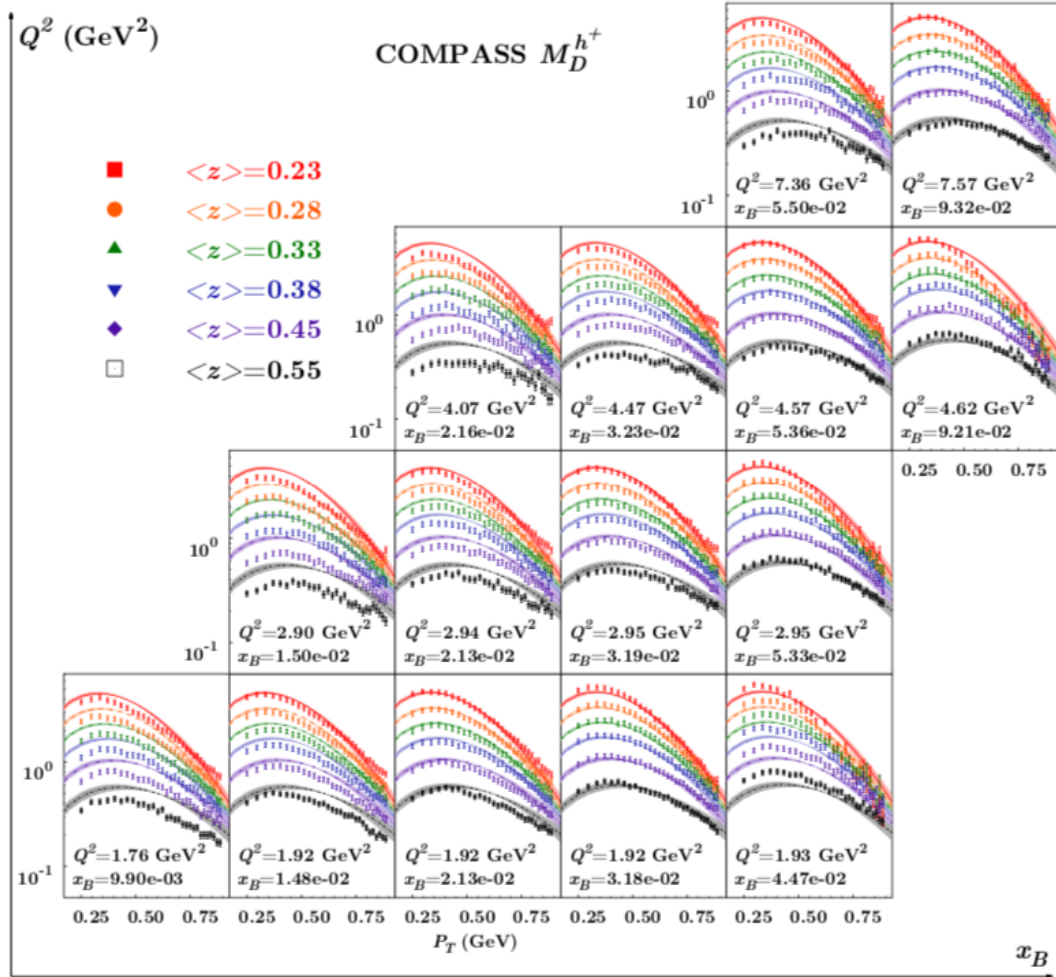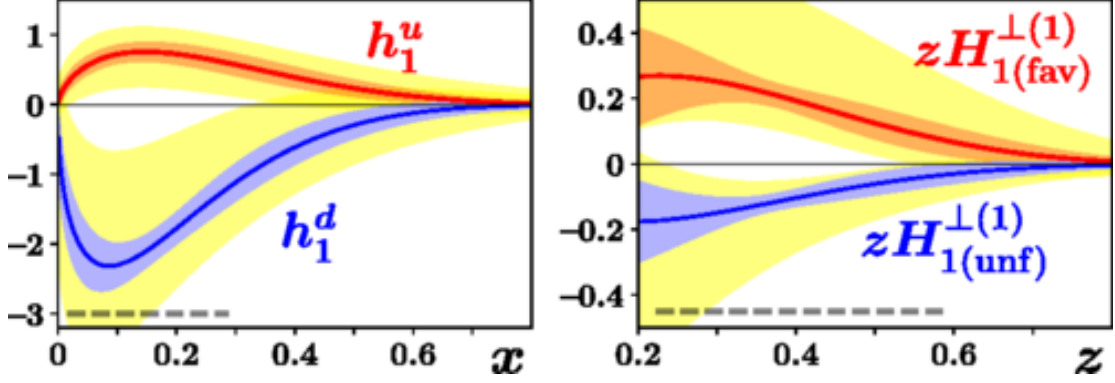
Fig. 1.7: COMPASS multiplicities fit using the Gaussian ansatz. COMPASS multiplicities described well by the Gaussian ansatz.

Fig. 1.8: The transversity TMD (left) and Collins FF (right) extracted by global
analysis of measurements at HERMES and COMPASS.

1.5.3 Transversity TMD

The Transversity TMD $h_1(x, k_\perp)$ is often extracted together with the Sivers TMD
$f_{1T}^\perp(x, k_\perp)$ as they can both be accessed by using a transversly polarized target
and measuring the target spin asymmetry defined below.

$$A_{UT}^h(\phi_h, \phi_S) = \frac{1}{s_\perp} \frac{d\sigma^h(\phi_h, \phi_S) - d\sigma^h(\phi_h, \phi_S + \pi)}{d\sigma^h(\phi_h, \phi_S) + d\sigma^h(\phi_h, \phi_S + \pi)} \tag{1.19}$$

Because of the coupling of transversity h_1 to the Collins fragmentation func-
tion (both chiral-odd), the asymmetry is often called the Collins asymmetry. The
full results are described in Ref. [13], where the HERMES collaboration observed
non-zero Collins asymmetries for charged pions and positively charged kaons.
Transversity was recently extracted simultaneously with the Collins fragmenta-
tion function in Ref. [14].
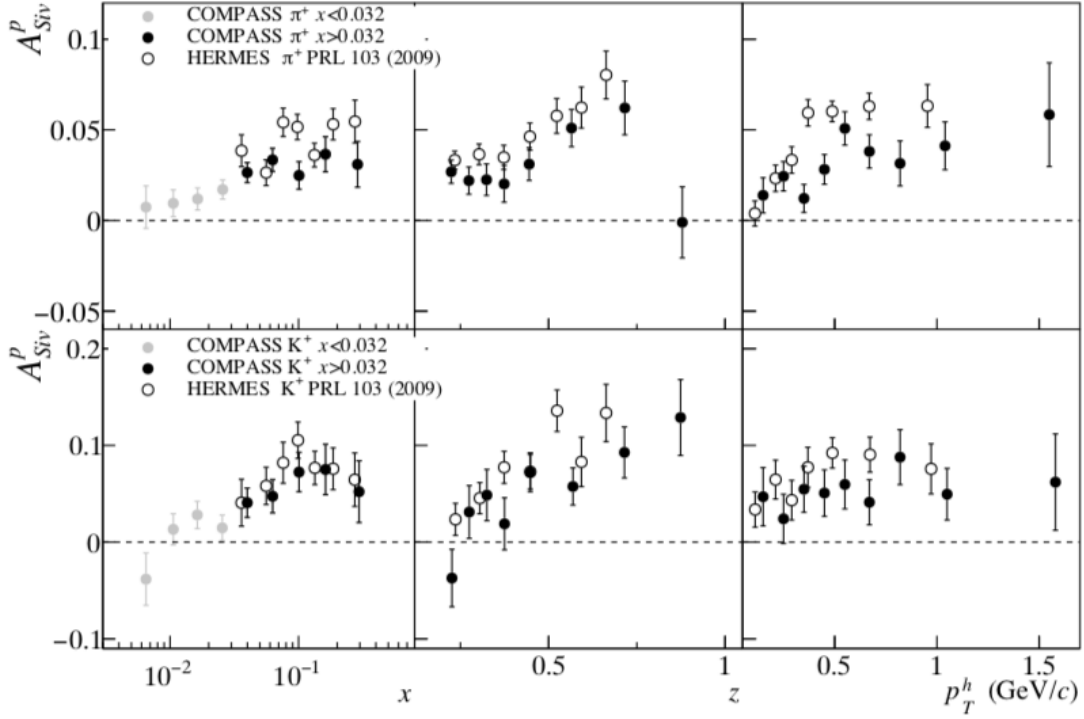
Fig. 1.9: The Sivers asymmetry measured at COMPASS and HERMES for different hadron species identified in the final state, demonstrating a clear non-zero effect.

1.5.4 Sivers TMD

Naively, one might throw away the Sivers function altogether for its time reversal oddity, given that the hadronic tensor $W^{\mu\nu}$ must be time reversal invariant. However, the Sivers asymmetry has been observed by Jlab Hall A, HERMES and COMPASS and it is non-trivially large [15], [16], owing to QCD interactions in the final state. Noteworthy for this thesis, the observed asymmetries were largest for K^+.

An important property of TMDs that hasn't been stated yet is universality; the non-perturbative functions shouldn't depend on the process used to probe

them. For both the Sivers and Boer-Mulders functions there exists a *modified universality*, because the functions are expected to appear with opposite signs in Drell-Yan and SIDIS processes.

1.5.5 Boer-Mulders TMD

Boer-Mulders, like Sivers, is time reversal odd. Measurements of unpolarized moments for $\cos\phi_h$ and $\cos(2\phi_h)$ from HERMES and COMPASS have been made available for extraction of Boer-Mulders. HERMES defined the observable as follows.

$$\langle\cos\phi_h\rangle = \frac{\int_0^{2\pi} \cos\phi_h d^5\sigma(x_B, Q^2, z, P_T, \phi_h)d\phi_h}{\int_0^{2\pi} d^5\sigma(x_B, Q^2, z, P_T, \phi_h)d\phi_h} \tag{1.20}$$

$$\langle\cos(2\phi_h)\rangle = \frac{\int_0^{2\pi} \cos(2\phi_h) d^5\sigma(x_B, Q^2, z, P_T, \phi_h)d\phi_h}{\int_0^{2\pi} d^5\sigma(x_B, Q^2, z, P_T, \phi_h)d\phi_h} \tag{1.21}$$

A twist-four contribution to both of these observables exists, known as the Cahn effect. The Cahn term is proportional to the unpolarized functions $f_1 D_1$. Although extractions of Boer-Mulders are not abundant, one study has reported extracting both Boer-Mulders and Cahn from the $\cos(2\phi_h)$ moments of HERMES and COMPASS [17]. The asymmetry is non-zero, and as the authors note, the uncertainty on Boer-Mulders is still quite large, and a multidimensional analysis of SIDIS would help in constraining the parameters.
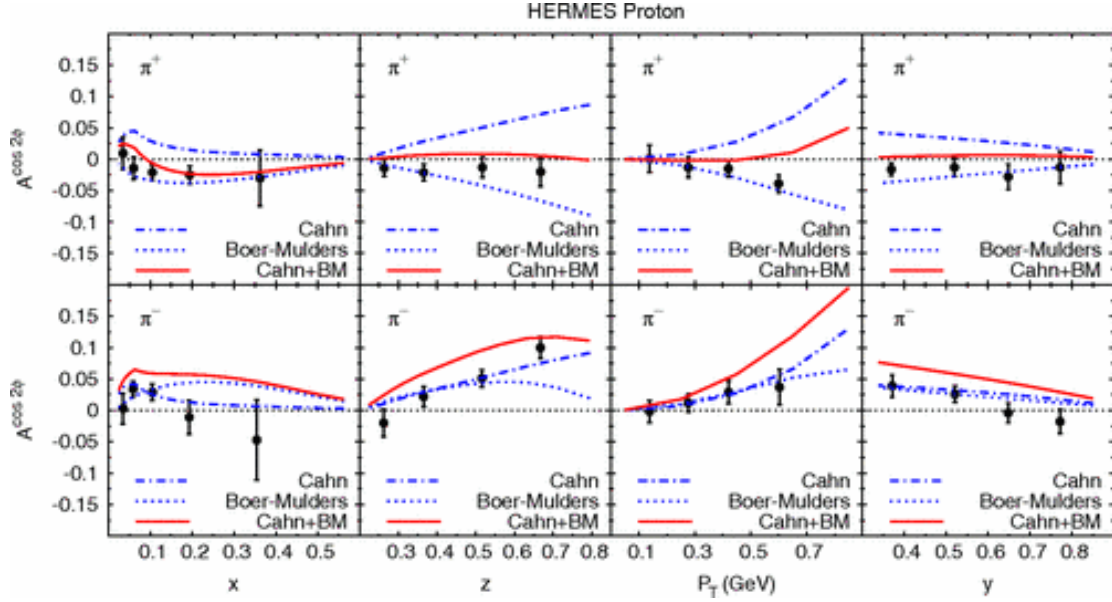
Fig. 1.10: The Boer-Mulders and Cahn effects extracted from HERMES data on the $\cos(2\phi_h)$ moment of SIDIS, reported in [17].

1.6 This Thesis

The unpolarized cross section for charged pions $(\pi^{\pm})$ is presented in chapter 7. This analysis extends the work of Nathan Harrison in his thesis work [18]. Our results for the cross section, useful in their own right (regardless of the framework used to explain the physics inside of structure functions), are a multidimensional measurement which can be used to constrain the Boer-Mulders and Cahn effects in the kinematics of Jefferson Lab.

In chapter 7, measurements of beam spin asymmetries (BSA) for positively charged k-mesons (kaons or K^+) are presented. The BSA is defined as,

$$BSA = \frac{d\sigma^+ - d\sigma^-}{d\sigma^+ + d\sigma^-} = \frac{A_{LU}^{\sin\phi_h}\sin\phi_h}{1 + A_{UU}^{\cos\phi_h}\cos\phi_h + A_{UU}^{\cos(2\phi_h)}\cos(2\phi_h)} \tag{1.22}$$

where the superscript $\pm$ refers to the helicity value λ_e and the coefficient $A_{LU}^{\sin\phi}$ is shown below.

$$A_{LU}^{\sin\phi} = \sqrt{2\,\varepsilon(1-\varepsilon)}\frac{F_{LU}^{\sin\phi}}{F_{UU,T} + \varepsilon F_{UU,L}} \tag{1.23}$$

The unpolarized coefficients are defined in a similar way.

$$A_{UU}^{\cos\phi_h} = \sqrt{2\varepsilon(1+\varepsilon)}\frac{F_{UU}^{\cos\phi_h}}{F_{UU,T} + \varepsilon F_{UU,L}} \tag{1.24}$$

$$A_{UU}^{\cos(2\phi_h)} = \varepsilon\frac{F_{UU}^{\cos(2\phi_h)}}{F_{UU,T} + \varepsilon F_{UU,L}} \tag{1.25}$$

There are several interesting motivations for this measurement. First, the TMD content of $F_{LU}^{\sin\phi}$ is purely twist-three. If twist-three contributions are vanishingly small at Jefferson Lab 6 GeV kinematics, the observed asymmetry should be zero. This was not the case for pions, as observed by Gohn [19]. Additionally, the magnitude of the Sivers effect for K^+ was surprisingly large, however in most other measurements K^+ signals have generally followed π^+ signals.

I have reviewed the experimental hardware that enables this thesis work in chapter 2 and summarized analytic techniques used during chapter 3. I describe basic analysis procedures that are common to both measurements in chapter 4 before discussing particle identification in chapter 5. I present results for the inclusive scattering cross section in chapter 6, followed by the SIDIS cross section in chapter 7. I then present my findings for the positively charged kaon BSA measurement in chapter 8 before offering a brief summary and outlook in chapter 9.

References

[1] R. Hofstadter and R. W. McAllister, Phys. Rev. **98**, 217 (1955).

[2] R. Hofstadter, Rev. Mod. Phys. **28**, 214 (1956).

[3] E. E. Chambers and R. Hofstadter, Phys. Rev. **103**, 1454 (1956).

[4] G. Zweig, (1964).

[5] J. D. Bjorken and E. A. Paschos, Phys. Rev. **185**, 1975 (1969).

[6] R. P. Feynman, Phys. Rev. Lett. **23**, 1415 (1969), [,494(1969)].

[7] P. J. Mulders and R. D. Tangerman, Nucl. Phys. **B461**, 197 (1996), [Erratum: Nucl. Phys.B484,538(1997)], arXiv:hep-ph/9510301 [hep-ph] .

[8] A. Bacchetta, M. Diehl, K. Goeke, A. Metz, P. J. Mulders, and M. Schlegel, JHEP **02**, 093 (2007), arXiv:hep-ph/0611265 [hep-ph] .

[9] J. Collins, Camb. Monogr. Part. Phys. Nucl. Phys. Cosmol. **32**, 1 (2011).

[10] A. Airapetian *et al.* (HERMES), Phys. Rev. **D87**, 074029 (2013), arXiv:1212.5407 [hep-ex] .

[11] M. Aghasyan *et al.* (COMPASS), Phys. Rev. **D97**, 032006 (2018), arXiv:1709.07374 [hep-ex] .

[12] M. Anselmino, M. Boglione, J. O. Gonzalez Hernandez, S. Melis, and A. Prokudin, JHEP **04**, 005 (2014), arXiv:1312.6261 [hep-ph] .

[13] A. Airapetian *et al.* (HERMES), Phys. Lett. **B693**, 11 (2010), arXiv:1006.4221 [hep-ex] .

[14] H.-W. Lin, W. Melnitchouk, A. Prokudin, N. Sato, and H. Shows, Phys. Rev. Lett. **120**, 152502 (2018), arXiv:1710.09858 [hep-ph] .

[15] C. Adolph *et al.* (COMPASS), Phys. Lett. **B744**, 250 (2015), arXiv:1408.4405 [hep-ex] .

[16] X. Qian *et al.* (Jefferson Lab Hall A), Phys. Rev. Lett. **107**, 072003 (2011), arXiv:1106.0363 [nucl-ex] .

[17] V. Barone, S. Melis, and A. Prokudin, Phys. Rev. **D81**, 114026 (2010), arXiv:0912.5194 [hep-ph] .

[18] N. A. Harrison, *Exploring the Structure of the Proton via Semi-Inclusive Pion Electroproduction*, Ph.D. thesis, Connecticut U. (2010).

[19] W. Gohn, *Probing the Proton's Quark Dynamics in Semi-inclusive Pion Electroproduction*, Ph.D. thesis, Connecticut U. (2012).